



TITLE:

# Natural Convection in an Enclosed Region (流体力学における混合境界値問題)

AUTHOR(S):

RASHID, KHALID

---

CITATION:

RASHID, KHALID. Natural Convection in an Enclosed Region (流体力学における混合境界値問題). 数理解析研究所講究録 1978, 335: 155-172

ISSUE DATE:

1978-10

URL:

<http://hdl.handle.net/2433/104198>

RIGHT:

## NATURAL CONVECTION IN AN ENCLOSED REGION

KHALID RASHID

DEPARTMENT OF APPLIED PHYSICS,  
FACULTY OF ENGINEERING,  
NAGOYA UNIVERSITY, NAGOYA

The effect of localised heating at different pressures and temperatures on flow patterns in a rectangular channel is studied numerically. The governing equations for conservation of mass, momentum, energy and equation of state for the problem are solved by using explicit finite difference scheme. All properties of the fluid, helium (He), are considered to be temperature dependent. The flow patterns at pressure greater than 50 mm Hg are found to be almost similar to that previously reported<sup>(1)</sup>.

### Introduction

Natural convection in enclosures has been receiving increasing attention in recent years because of the wide applications of this problem in everyday life, such as home-heating, cryogenic storage, thermal insulation and in the industry such as in furnace and nuclear designs. Theoretical studies of the problem

has also of significant importance as experimental, since its mathematical formulation leads to a set of non-linear partial differential equations. The solution of which even in numerical form is a difficult task.

Recently, Yatsuya et al.<sup>(1)</sup> considered the problem on "Formation of Ultrafine Metal Particles by Gas-Evaporation Technique", and flow patterns are reported. The flow patterns are discussed only on the basis of experimental results and no comparison is made with theoretical predictions. In spite of its industrial importance this problem has been given scant attention and no numerical solution is available yet.

The main purpose of this study is to present numerical solution for "Natural Convection in an Enclosed Region", and furthermore, to understand the role of certain key features of the flow patterns reported in the experimental study by Yatsuya et al.<sup>(1)</sup>.

In most of previous studies<sup>(2,3,4)</sup> on convection problems, Boussinesque approximation was frequently used. This approximation is very useful when temperature differences involved are small, i.e., vertical density variation are small. However, for problems as in astrophysics, meteorology and the present study where the temperature differences are very large, this approximation may lead to erroneous results. Therefore, the basic differential equations for the problem considered are numerically solved with variable fluid properties, thermal conductivity,  $\kappa$ , and viscosity,  $\mu$ .

### Formulation of the problem

The geometry of the problem is sketched in Figure 1. Cartesian co-ordinate  $(x,y)$  is introduced with origin at the centre of the base of the outer duct. The size and location of the heated duct (inner) is considered to be variable. The fluid, He, is initially motionless at a uniform room temperature,  $T_c$ . Helium gas which is compressible and viscous is assumed to behave as an ideal gas. The properties of the fluid, thermal conductivity,  $\kappa$ , and viscosity,  $\mu$ , are assumed to be temperature dependent and independent of pressure.

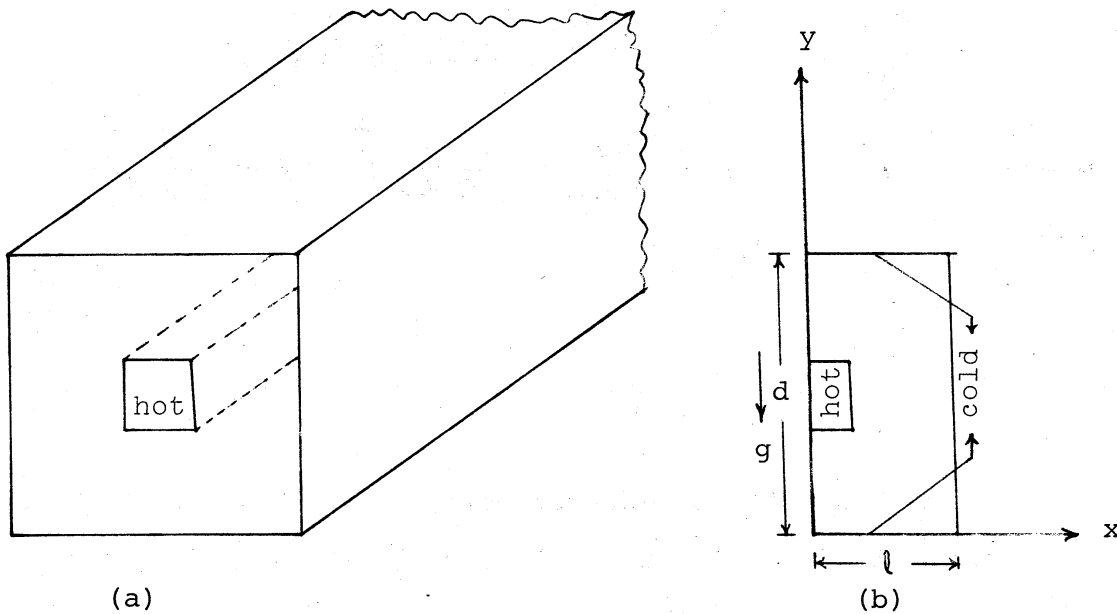


Figure 1. Rectangular enclosure and co-ordinate system

The steady-state governing equations for the conservation of mass, momentum and energy with an equation of state, plus the expressions for thermal conductivity and viscosity are expressed as

$$\frac{\partial(\rho V_\beta)}{\partial(x_\beta)} = 0, \quad \beta = 1, 2 \quad (1)$$

$$\rho V_\beta \frac{\partial V_\alpha}{\partial x_\beta} = -\frac{\partial p}{\partial x_\alpha} + \frac{\partial}{\partial x_\beta} \left[ \mu \left( \frac{\partial V_\beta}{\partial x_\alpha} + \frac{\partial V_\alpha}{\partial x_\beta} \right) \right] - \frac{2}{3} \frac{\partial}{\partial x_\alpha} \left( \mu \frac{\partial V_\beta}{\partial x_\beta} \right) + \rho F_\alpha \quad (2)$$

where  $F_\alpha$  is the external force.

$$\rho C_v V_\beta \frac{\partial T}{\partial x_\beta} = \Phi - p\theta + \frac{\partial}{\partial x_\beta} \left( \kappa \frac{\partial T}{\partial x_\beta} \right) \quad (3)$$

where  $\Phi = \frac{1}{2} \mu \left( \frac{\partial V_\alpha}{\partial x_\beta} + \frac{\partial V_\beta}{\partial x_\alpha} \right)^2 - \frac{2}{3} \mu \left( \frac{\partial V_\beta}{\partial x_\beta} \right)^2$

and

$$\theta = \frac{\partial V_\beta}{\partial x_\beta} \quad (4)$$

$$p = \frac{R}{m} \rho T \quad (5)$$

Thermal conductivity and viscosity with variation in temperature may satisfactorily be estimated by the following equations

$$\kappa = a_0 + a_1 T + a_2 T^2 \quad (6)$$

$$\mu = c_0 + c_1 T + c_2 T^2 \quad (7)$$

These equations are based on the experimental results<sup>(5,6)</sup> fitted by least square method and are shown in Figures (2-a) and (2-b), respectively.

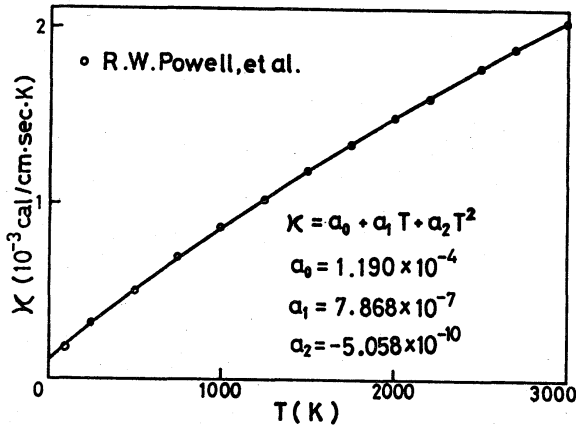


Figure 2-a. Variation of thermal conductivity with temperature.

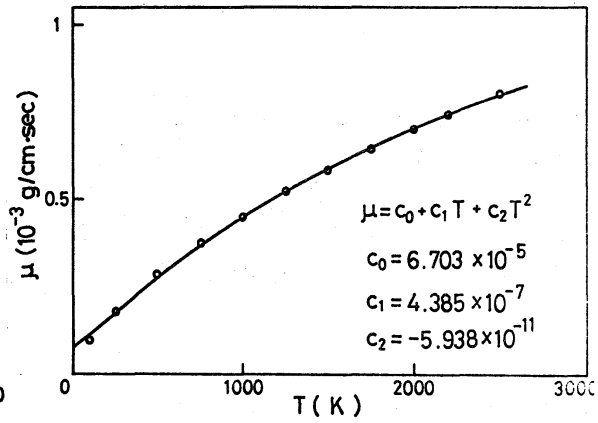


Figure 2-b. Variation of viscosity with temperature.

In equations (2), (3) and (5), pressure can be written as

$$p = p_s + p_d \quad (8)$$

To get a suitable form of a set of equations for computation, the following steps are adopted.

i) introduce a stream function,  $\psi$ , and vorticity vector,  $\omega$ , as

$$\rho u = \frac{\partial \psi}{\partial y} \quad (9)$$

$$\rho v = -\frac{\partial \psi}{\partial x} \quad (10)$$

$$\omega = \frac{\partial v}{\partial x} - \frac{\partial u}{\partial y} \quad (11)$$

where  $u$  and  $v$  are the velocity components along the  $x$  and  $y$ -axis.

Equations (9) and (10) satisfy the equation of continuity.

ii) take the rotation (curl) of equation (2) to eliminate the pressure term.

iii) take the divergence of equation (2).

After applying the above steps, a set of equations can be written as

$$\frac{1}{\rho} \nabla^2 \psi = \frac{1}{\rho^2} \nabla \rho \cdot \nabla \psi - \omega \quad (12)$$

$$\begin{aligned} \mu \nabla^2 \omega = & -\frac{\partial(\psi, \omega)}{\partial(x, y)} + \frac{1}{\rho^2} \left( \frac{\partial \psi}{\partial x} \frac{\partial(\rho, \frac{\partial \psi}{\partial x})}{\partial(x, y)} + \frac{\partial \psi}{\partial y} \frac{\partial(\rho, \frac{\partial \psi}{\partial y})}{\partial(x, y)} \right) \\ & - 2 \left[ \nabla \mu \nabla \omega + \frac{\partial(\mu, \theta)}{\partial(x, y)} + \frac{1}{\rho^2} \left( \frac{\partial(\rho, \frac{\partial \mu}{\partial x})}{\partial(x, y)} \frac{\partial \psi}{\partial y} - \frac{\partial(\rho, \frac{\partial \mu}{\partial y})}{\partial(x, y)} \frac{\partial \psi}{\partial x} \right) \right. \\ & \left. + \frac{1}{\rho} \left( \frac{\partial(\frac{\partial \psi}{\partial x}, \frac{\partial \mu}{\partial y})}{\partial(x, y)} - \frac{\partial(\frac{\partial \psi}{\partial y}, \frac{\partial \mu}{\partial x})}{\partial(x, y)} \right) \right] - \omega \nabla^2 \mu + g \frac{\partial \rho}{\partial x} \quad (13) \end{aligned}$$

$$\begin{aligned} \nabla^2 p_d = & \left[ \frac{\partial(\psi, \theta)}{\partial(x, y)} + \frac{2}{\rho} \frac{\partial(\frac{\partial \psi}{\partial x}, \frac{\partial \psi}{\partial y})}{\partial(x, y)} + \frac{1}{\rho^2} \left( \frac{\partial(\rho, \frac{\partial \psi}{\partial x})}{\partial(x, y)} \frac{\partial \psi}{\partial y} - \frac{\partial(\rho, \frac{\partial \psi}{\partial y})}{\partial(x, y)} \frac{\partial \psi}{\partial x} \right) \right] \\ & + \frac{4}{3} (\mu \nabla^2 \theta + \theta \nabla^2 \mu + 2 \nabla \mu \nabla \theta) - 2 \left[ \frac{\partial(\mu, \omega)}{\partial(x, y)} \right. \\ & - \frac{1}{\rho^2} \left( \frac{\partial(\rho, \frac{\partial \psi}{\partial x})}{\partial(x, y)} \frac{\partial \psi}{\partial x} + \frac{\partial(\rho, \frac{\partial \mu}{\partial y})}{\partial(x, y)} \frac{\partial \psi}{\partial y} \right) + \frac{1}{\rho} \left( \frac{\partial(\frac{\partial \psi}{\partial x}, \frac{\partial \mu}{\partial x})}{\partial(x, y)} + \right. \\ & \left. \left. \frac{\partial(\frac{\partial \psi}{\partial y}, \frac{\partial \mu}{\partial y})}{\partial(x, y)} \right) \right] - g \frac{\partial \rho}{\partial y} \quad (14) \end{aligned}$$

$$\begin{aligned} K \nabla^2 T = & - \left[ c_v \frac{\partial(\psi, T)}{\partial(x, y)} - (p_s + p_d) \theta + \nabla K \nabla T + \frac{4}{3} \mu \theta^2 + \mu \omega^2 \right. \\ & \left. + \frac{4\mu}{\rho^2} \left\{ -\frac{\partial(\frac{\partial \psi}{\partial x}, \frac{\partial \psi}{\partial y})}{\partial(x, y)} + \frac{1}{\rho} \left( \frac{\partial(\rho, \frac{\partial \psi}{\partial y})}{\partial(x, y)} \frac{\partial \psi}{\partial x} - \frac{\partial(\rho, \frac{\partial \psi}{\partial x})}{\partial(x, y)} \frac{\partial \psi}{\partial y} \right) \right\} \right] \quad (15) \end{aligned}$$

$$\Theta = -\frac{1}{\rho^2} \frac{\partial(\rho, \psi)}{\partial(x, y)} \quad (16)$$

$$p_s + p_d = \frac{R}{m} \rho T \quad (17)$$

With boundary conditions

$$x=0, \begin{cases} 0 \leq y < y_e \\ y_f < y \leq d \end{cases} \quad \left. \begin{aligned} \psi=0 &= \frac{\partial \psi}{\partial x}, \quad \frac{\partial T}{\partial x} = 0 = \frac{\partial p_d}{\partial x}, \quad \omega=0 \end{aligned} \right\} \quad (18a)$$

$$x=x_g, y_e \leq y \leq y_f: \quad \left. \begin{aligned} \psi=0 &= \frac{\partial \psi}{\partial x}, \quad \omega = -\frac{1}{\rho} \frac{\partial^2 \psi}{\partial x^2} \\ \frac{\partial p}{\partial x} &= \frac{4}{3} \mu \frac{\partial \Theta}{\partial x} - \mu \frac{\partial \omega}{\partial y} + \omega \frac{\partial \mu}{\partial y}, \quad T = T_h \end{aligned} \right\} \quad (18b)$$

$$x=l, \text{ for all } y: \quad \left. \begin{aligned} \psi=0 &= \frac{\partial \psi}{\partial x}, \quad \omega = -\frac{1}{\rho} \frac{\partial^2 \psi}{\partial x^2} \\ \frac{\partial p}{\partial x} &= \frac{4}{3} \mu \frac{\partial \Theta}{\partial x} - \mu \frac{\partial \omega}{\partial y} + \omega \frac{\partial \mu}{\partial y}, \quad T = T_c \end{aligned} \right\} \quad (18c)$$

$$y=0 \text{ and } y=d, \text{ for all } x: \quad \left. \begin{aligned} \psi=0 &= \frac{\partial \psi}{\partial y}, \quad \omega = -\frac{1}{\rho} \frac{\partial^2 \psi}{\partial y^2} \\ \frac{\partial p}{\partial y} &= \frac{4}{3} \mu \frac{\partial \Theta}{\partial y} + \mu \frac{\partial \omega}{\partial x} - \omega \frac{\partial \mu}{\partial x} - g\rho \\ T &= T_c \end{aligned} \right\} \quad (18d)$$

$$\begin{aligned} y=y_e \text{ and } y=y_f; \quad 0 \leq x \leq x_g: \quad & \left. \begin{aligned} \psi=0 &= \frac{\partial \psi}{\partial y}, \quad \omega = -\frac{1}{\rho} \frac{\partial^2 \psi}{\partial y^2} \\ \frac{\partial p}{\partial y} &= \frac{4}{3} \mu \frac{\partial \Theta}{\partial y} + \mu \frac{\partial \omega}{\partial x} - \omega \frac{\partial \mu}{\partial x} - g\rho \\ T &= T_h \end{aligned} \right\} \quad (18e) \end{aligned}$$

Equations (12) through (17) can be put in dimensionless form as

$$\frac{1}{\rho'} \nabla^2 \Psi = \frac{1}{\rho'^2} \nabla \rho' \cdot \nabla \Psi - \Omega \quad (19)$$



$$\begin{aligned} \mu' \nabla^2 \Omega = \text{Re} \left[ -\frac{\partial(\psi, \Omega)}{\partial(x', y')} + \frac{1}{\rho'} \left( \frac{\partial\psi}{\partial x'} \frac{\partial(\rho', \frac{\partial\psi}{\partial x'})}{\partial(x', y')} + \frac{\partial\psi}{\partial y'} \frac{\partial(\rho', \frac{\partial\psi}{\partial y'})}{\partial(x', y')} \right) \right] \\ - 2 \left[ \nabla \mu' \nabla \Omega + \frac{\partial(\mu', \theta')}{\partial(x', y')} + \frac{1}{\rho'^2} \left( \frac{\partial(\rho', \frac{\partial\mu'}{\partial x'})}{\partial(x', y')} \frac{\partial\psi}{\partial y'} - \frac{\partial(\rho', \frac{\partial\mu'}{\partial y'})}{\partial(x', y')} \frac{\partial\psi}{\partial x'} \right) \right. \\ \left. + \frac{1}{\rho'} \left( \frac{\partial(\frac{\partial\psi}{\partial x'}, \frac{\partial\mu'}{\partial y'})}{\partial(x', y')} - \frac{\partial(\frac{\partial\psi}{\partial y'}, \frac{\partial\mu'}{\partial x'})}{\partial(x', y')} \right) \right] - \Omega \nabla^2 \mu' + \frac{\text{Re}}{\text{Fr}} \frac{\partial \rho'}{\partial x'} \quad (20) \end{aligned}$$

$$\begin{aligned} \nabla^2 \rho' = \left[ \frac{\partial(\psi, \theta')}{\partial(x', y')} + \frac{2}{\rho'} \frac{\partial(\frac{\partial\psi}{\partial x'}, \frac{\partial\psi}{\partial y'})}{\partial(x', y')} + \frac{1}{\rho'^2} \left( \frac{\partial(\rho', \frac{\partial\psi}{\partial x'})}{\partial(x', y')} \frac{\partial\psi}{\partial y'} - \frac{\partial(\rho', \frac{\partial\psi}{\partial y'})}{\partial(x', y')} \frac{\partial\psi}{\partial x'} \right) \right. \\ \left. + \frac{1}{\text{Re}} \left[ \frac{4}{3} (\mu' \nabla^2 \theta' + \theta' \nabla^2 \mu' + 2 \nabla \mu' \nabla \theta' - 2 \left\{ \frac{\partial(\mu', \Omega)}{\partial(x', y')} - \frac{1}{\rho'} \left( \frac{\partial(\rho', \frac{\partial\mu'}{\partial x'})}{\partial(x', y')} \frac{\partial\psi}{\partial x'} + \frac{\partial(\rho', \frac{\partial\mu'}{\partial y'})}{\partial(x', y')} \frac{\partial\psi}{\partial y'} \right) + \frac{1}{\rho'} \left( \frac{\partial(\frac{\partial\psi}{\partial x'}, \frac{\partial\mu'}{\partial x'})}{\partial(x', y')} \right. \right. \right. \right. \right. \\ \left. \left. \left. + \frac{\partial(\frac{\partial\psi}{\partial y'}, \frac{\partial\mu'}{\partial y'})}{\partial(x', y')} \right) \right\} \right] - \frac{1}{\text{Fr}} \frac{\partial \rho'}{\partial y'} \right] \quad (21) \end{aligned}$$

$$\begin{aligned} K' \nabla^2 T' = - \left[ \frac{\text{Pr} \cdot \text{Re}}{\gamma} \frac{\partial(\psi, T')}{\partial(x', y')} - \frac{\gamma-1}{\gamma} \text{Pr} \cdot \text{Re} \theta' - (\gamma-1) \text{Pr} \cdot \text{Re} M^2 \rho' \theta' \right. \\ \left. + \nabla K' \cdot \nabla T' + (\gamma-1) M^2 \text{Pr} \mu' \left[ \Omega^2 + \frac{4}{3} \theta'^2 + \frac{4}{\rho'^2} \left\{ -\frac{\partial(\frac{\partial\psi}{\partial x'}, \frac{\partial\psi}{\partial y'})}{\partial(x', y')} \right. \right. \right. \right. \\ \left. \left. \left. + \frac{1}{\rho'} \left( \frac{\partial(\rho', \frac{\partial\psi}{\partial y'})}{\partial(x', y')} \frac{\partial\psi}{\partial x'} - \frac{\partial(\rho', \frac{\partial\psi}{\partial x'})}{\partial(x', y')} \frac{\partial\psi}{\partial y'} \right) \right\} \right] \right] \quad (22) \end{aligned}$$

$$\rho' = (1 + \gamma M^2 \rho') / T' \quad (23)$$

$$\theta' = -\frac{1}{\rho'^2} \frac{\partial(\rho', \psi)}{\partial(x', y')} \quad (24)$$

$$K' = a_0 + a_1 T' + a_2 T'^2 \quad (25)$$

$$\mu' = c_0 + c_1 T' + c_2 T'^2 \quad (26)$$

$$\begin{aligned} a_0 = \frac{a_0}{1}, \quad a_1 = \frac{a_1 T}{K_1}, \quad a_2 = \frac{a_2 T^2}{K_1} \\ c_0 = \frac{c_0}{\mu_1}, \quad c_1 = \frac{c_1 T}{\mu_1}, \quad c_2 = \frac{c_2 T^2}{\mu_1} \end{aligned}$$

boundary conditions are

$$x' = 0, \left. \begin{matrix} 0 \leq y' < y_e \\ y_f < y' < 1 \end{matrix} \right\} : \quad \psi = 0 = \frac{\partial^2 \psi}{\partial x'^2}, \quad \frac{\partial T'}{\partial x'} = 0 = \frac{\partial p'}{\partial x'}, \quad \Omega = 0 \quad (27a)$$

$$x' = x_g, \quad y_e \leq y' < y_f \left\{ \begin{array}{l} \psi = 0 = \frac{\partial \psi}{\partial x'}, \quad \Omega = -\frac{1}{\rho'} \frac{\partial^2 \psi}{\partial x'^2} \\ \frac{\partial p'}{\partial x'} = \frac{1}{Re} \left( \frac{4}{3} \mu' \frac{\partial \theta'}{\partial x'} - \mu' \frac{\partial \Omega}{\partial y'} + \Omega \frac{\partial \mu'}{\partial y'} \right) \\ T' = \eta \end{array} \right. \quad (27b)$$

$$x' = 1, \text{ for all } y' : \left\{ \begin{array}{l} \psi = 0 = \frac{\partial \psi}{\partial x'}, \quad \Omega = -\frac{1}{\rho'} \frac{\partial^2 \psi}{\partial x'^2} \\ \frac{\partial p'}{\partial x'} = \frac{1}{Re} \left( \frac{4}{3} \mu' \frac{\partial \theta'}{\partial x'} - \mu' \frac{\partial \Omega}{\partial y'} + \Omega \frac{\partial \mu'}{\partial y'} \right) \\ T' = 1. \end{array} \right. \quad (27c)$$

$$y' = 0 \text{ and } y' = f; \text{ for all } x' : \left\{ \begin{array}{l} \psi = 0 = \frac{\partial \psi}{\partial y'}, \quad \Omega = -\frac{1}{\rho'} \frac{\partial^2 \psi}{\partial y'^2} \\ \frac{\partial p'}{\partial y'} = \frac{1}{Re} \left( \frac{4}{3} \mu' \frac{\partial \theta'}{\partial y'} + \mu' \frac{\partial \Omega}{\partial x'} - \Omega \frac{\partial \mu'}{\partial x'} \right) - \frac{\rho'}{Fr} \\ T' = 1. \end{array} \right. \quad (27d)$$

$$y' = y_e \text{ and } y' = y_f; \quad 0 \leq x' < x_g : \left\{ \begin{array}{l} \psi = 0 = \frac{\partial \psi}{\partial y'}, \quad \Omega = -\frac{1}{\rho'} \frac{\partial^2 \psi}{\partial y'^2} \\ \frac{\partial p'}{\partial y'} = \frac{1}{Re} \left( \frac{4}{3} \mu' \frac{\partial \theta'}{\partial y'} + \mu' \frac{\partial \Omega}{\partial x'} - \Omega \frac{\partial \mu'}{\partial x'} \right) - \frac{\rho'}{Fr} \\ T' = \eta \end{array} \right. \quad (27e)$$

#### Finite difference approximation and numerical solution

The numerical method employed in this study is based on straightforward explicit finite difference scheme. The enclosure is divided into a finite number of grids having equal width along

two axes. Then an approximation is made at all the grid points having the co-ordinates  $x=i\Delta x$  and  $y=j\Delta y$ , where  $i$  and  $j$  are integers. Applying the Taylor's series expansion to the variables at a point  $(i,j)$ , we may obtain the approximation

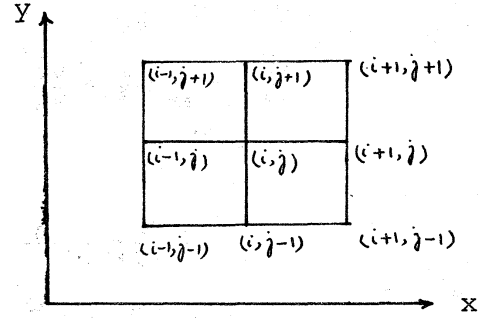


Figure 3. Arrangement of grid points

$$\frac{\partial f}{\partial x} = \frac{f(i+1, j) - f(i, j)}{\Delta x} \quad (28)$$

$$\frac{\partial f}{\partial x} = \frac{f(i, j) - f(i-1, j)}{\Delta x} \quad (29)$$

$$\frac{\partial f}{\partial x} = \frac{f(i+1, j) - f(i-1, j)}{2 \Delta x} \quad (30)$$

$$\frac{\partial^2 f}{\partial x^2} = \frac{f(i+1, j) - 2f(i, j) + f(i-1, j)}{(\Delta x)^2} \quad (31a)$$

Equations (28), (29) and (30) are known as the forward, backward and central finite difference forms, respectively, at  $(i, j)$ . The central finite difference is used in the enclosure where

backward and forward difference schemes are applied at the boundaries. Similar forms exist for the derivative with respect to  $y$ . It may also be shown

$$\frac{\partial^2 f}{\partial x \partial y} = \frac{f(i+1, j+1) - f(i-1, j+1) - f(i+1, j-1) + f(i-1, j-1)}{4 \Delta x \Delta y} \quad (31b)$$

The procedure for numerical solution of a set of Equations (19) through (24) after linearization with help of Equations (28) to (31), is given in Figure 4.

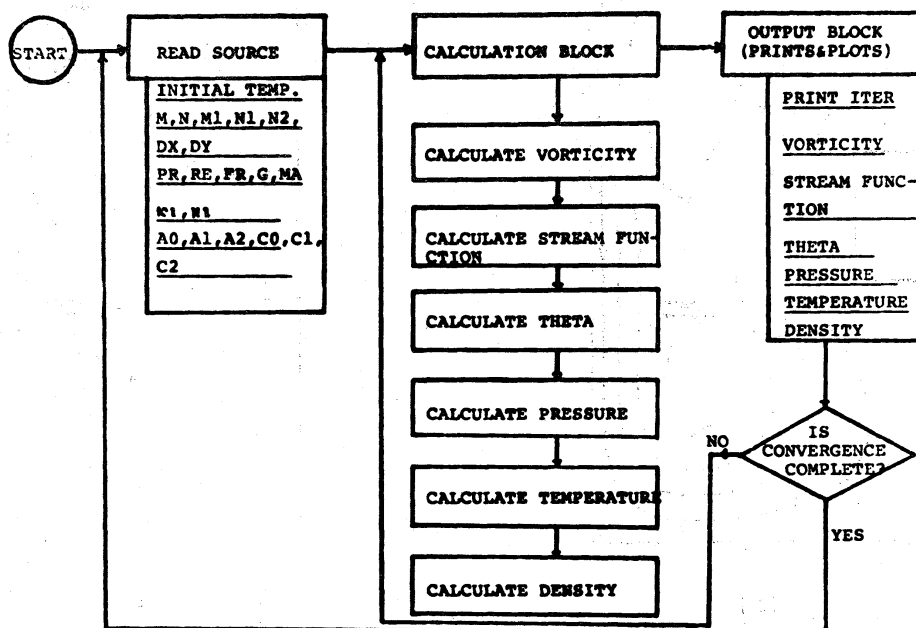


Figure 4. Flow chart for temperature distribution and flowfield.

## Results and Discussion

Figure 5 shows that the fluid flow is surprisingly complex, consisting of two individual anticlockwise eddies in the upper and lower parts of the enclosure with the inner duct one fifth of the outer duct. It seems at such a higher temperature the boundary layer flow is well established at the strong vorticity near the wall is able to sustain a weak return motion in the outer part of the boundary layer. Moreover, this figure shows that in the region of return flow the opposite boundary layer

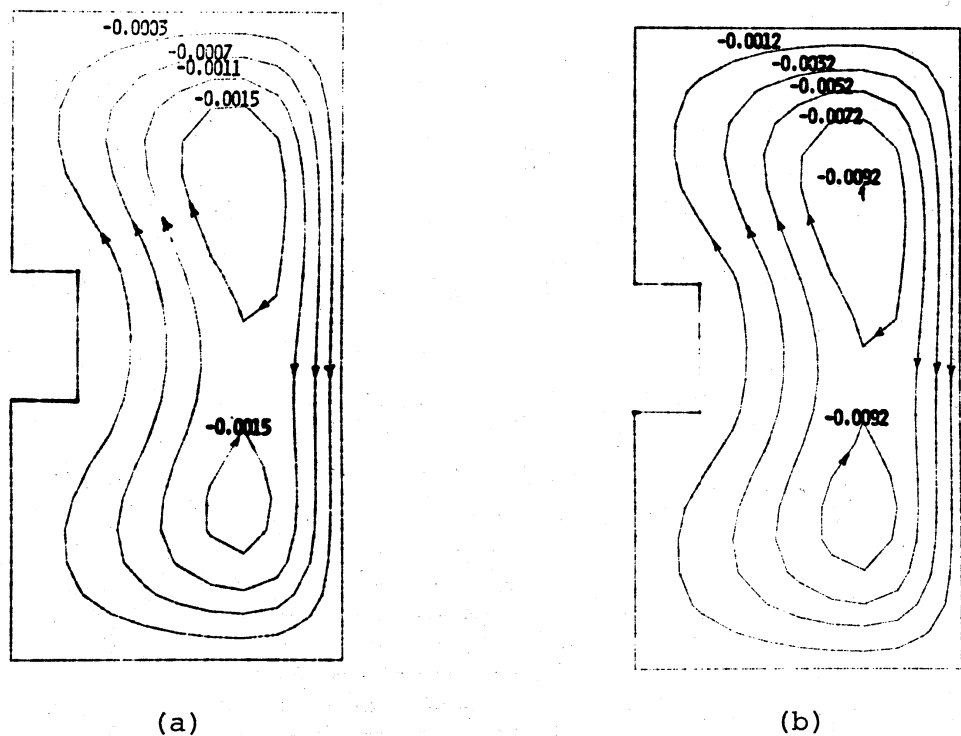


Figure 5. Streamlines at (a)  $Re=4.9$  (10 mm Hg) and temperature  $1300\text{ }^{\circ}\text{C}$  (b)  $Re=24.0$  (50 mm Hg) and temperature  $1300\text{ }^{\circ}\text{C}$ .

has almost no influence on the flow.

Figure 6 indicates the effect of temperature at constant pressure. The minimum value of the stream function increases with the decrease in temperature of the inner duct. Moreover, at low pressure, streamlines move a little away from the centre line toward the right hand wall. These results are obtained with the flat inner duct (heating element).

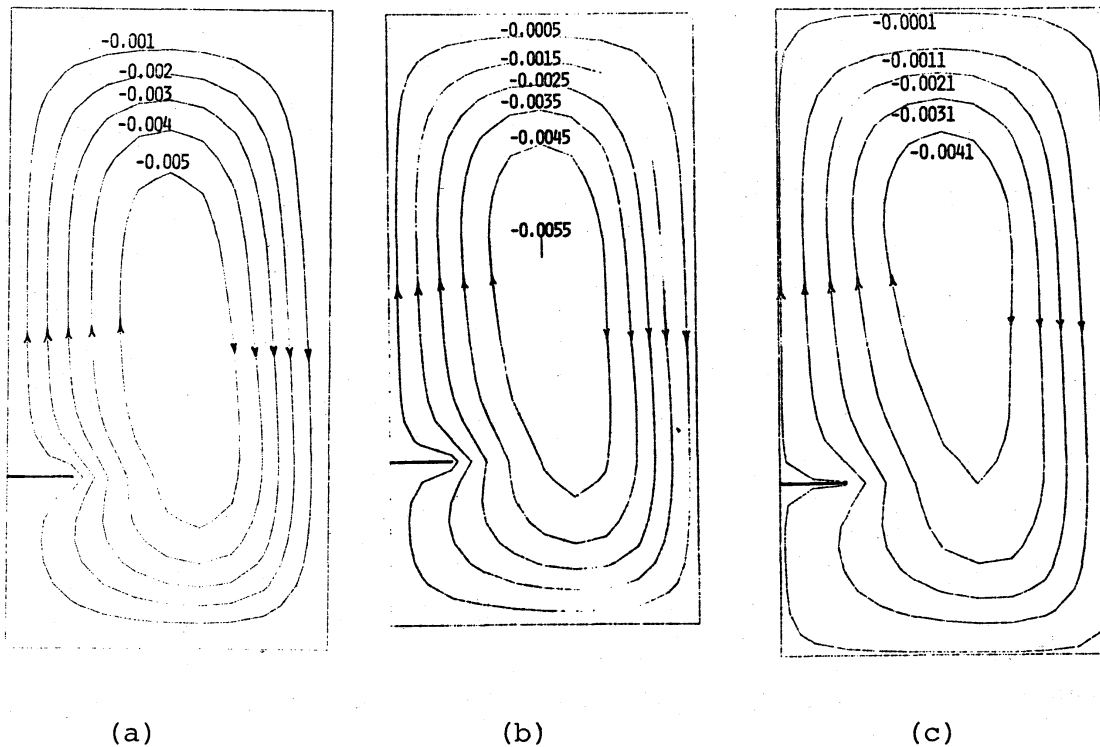


Figure 6. Streamlines at pressure 10 mm Hg (a)  $Re=6.56$   $T_h=1100$  °C (b)  $Re=6.04$   $T_h=1300$  °C (c)  $Re=5.58$   $T_h=1500$  °C.

When the numerical results are compared with the existing experimental results<sup>(1)</sup>, it is found that the theoretical flow patterns are not exactly the same experienced in the experiments, especially at low pressure. This discrepancy may be attributed to the presence of metal. That is, as the metal evaporates at low

pressures, the change in the density gradients become large and thus affect the flow patterns. However, the numerical results agree satisfactorily at pressure above 50 mm Hg as shown in Figure 7. At such higher pressures gravity force is dominant

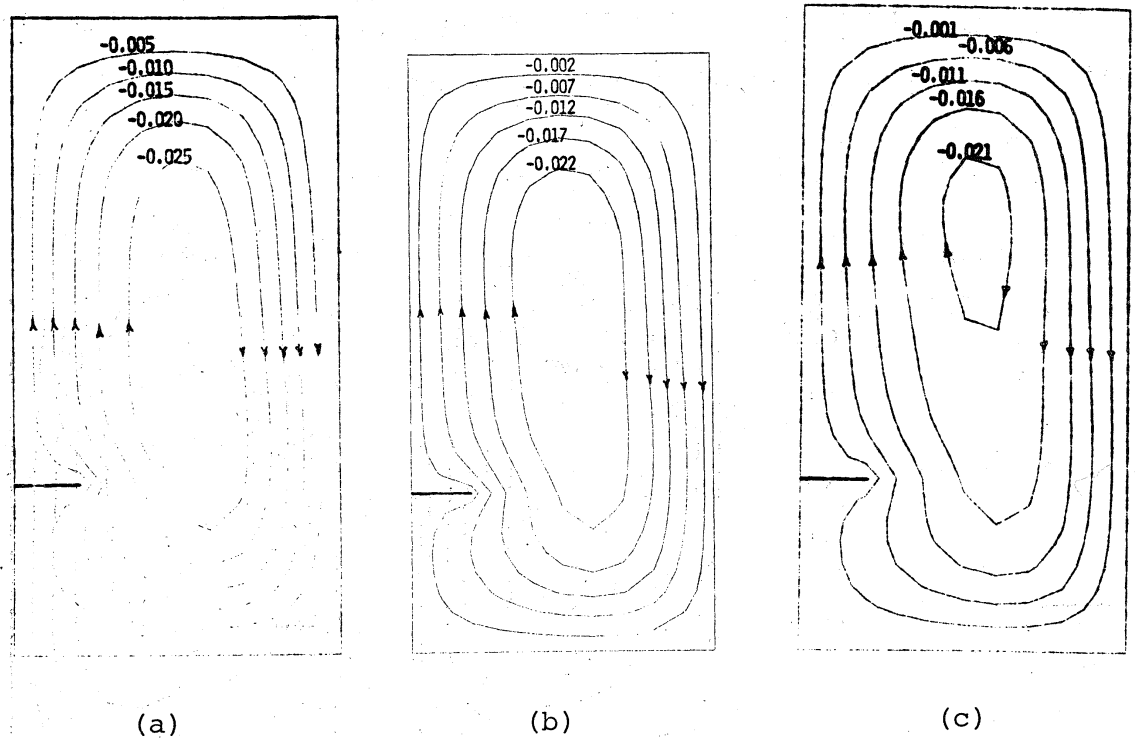


Figure 7. Streamlines at pressure 50 mm Hg (a)  $Re=32.0$   $T_h=1100$  °C (b)  $Re=30.19$   $T_h=1300$  °C (c)  $Re=27.90$   $T_h=1500$  °C.

which brings the flow directly up to the ceiling due to convection and then returns back due to the boundary.

Temperature distributions are illustrated in Figure 8. It is quite apparent from these figures that the temperature of heater and pressure have remarkable effect on the temperature distributions.

Figures 9 shows variation of pressure deviations from the

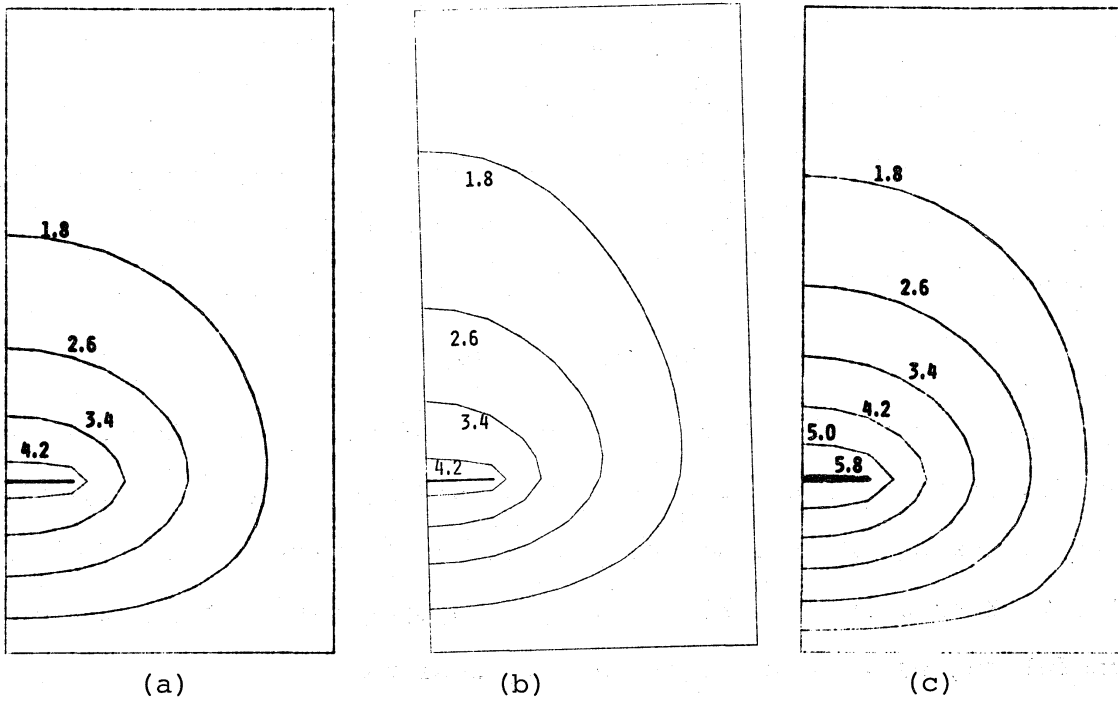


Figure 8. Temperature distributions at (a)  $Re=6.56$  (10 mm Hg)  $T_h=1100$  °C (b)  $Re=32.0$  (50 mm Hg)  $T_h=1100$  °C (c)  $Re=5.58$  (10 mm Hg)  $T_h=1500$  °C.

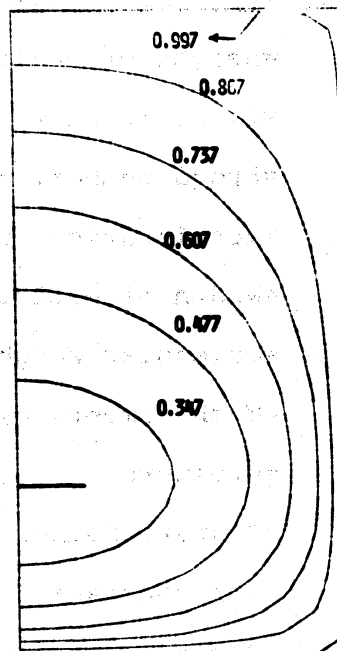
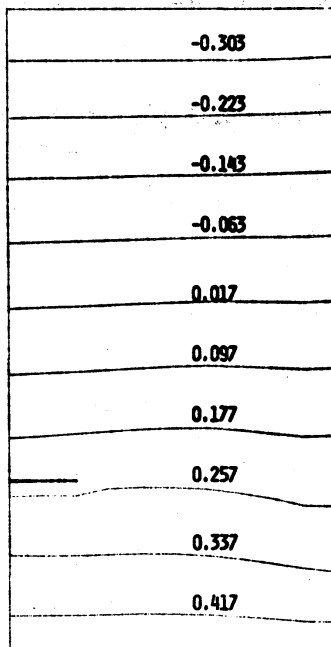


Figure 9. Pressure deviation from static pressure at  $Re=6.56$  (10 mm Hg)  $T_h=1100$  °C. Figure 10. Density distribution at  $Re=6.56$  (10 mm Hg)  $T_h=1100$  °C.



static pressure. There is apparently no variation in pressure, i.e., total pressure remains constant.

Figure 10 presents density distributions. This is the fact that with an increase in temperature, density decreases as is given by Equation (23).

#### Acknowledgements

The author is highly indebted to Professor Sinzi Kuwabara, of Nagoya University, for his solid guidance and proper supervision during the course of this study. Thanks are also due to Dr. Y. Kaneda and Dr. S. Yatsuya of Nagoya University, for their useful suggestions and critical discussions.

#### Nomenclature

$a_0, a_1, a_2$	=arbitrary constants as appeared in Eqs. (6) and (25)
$c_0, c_1, c_2$	=arbitrary constants as appeared in Eqs. (7) and (26)
$d$	=height of enclosure
$c_v, c_p$	=specific heats at constant volume and pressure, respectively
$Fr$	=Froud number, $=V^2/g\ell$
$g$	=acceleration due to gravity
	=width of enclosure
$m$	=molecular weight
$M$	=Mach number, $=\sqrt{gdm/\gamma Rt}$
$p$	=pressure
$Pr$	=Prandtl number, $=c_p\mu/\kappa$
$R$	=gas constant
$Re$	=Reynolds number, $=\rho_m V\ell/\mu$
$T$	=temperature

$u$	=horizontal component of velocity
$v$	=vertical component of velocity
$V$	=characteristic velocity, $=\sqrt{gd}$
$x$	=horizontal co-ordinate
$x'$	=dimensionless horizontal co-ordinate, $=x/l$
$y$	=vertical co-ordinate
$y'$	=dimensionless vertical co-ordinate, $=y/l$

## Greek symbols

$\Delta x$	=grid spacing in the x direction
$\Delta y$	=grid spacing in the y direction
$\nabla^2$	=Laplacian operator, $=\partial^2/\partial x^2 + \partial^2/\partial y^2$
$\kappa$	=thermal conductivity
$\kappa_1$	=thermal conductivity at maximum temperature
$\rho$	=density
$\rho'$	=dimensionless density, $=\rho/\rho_m$
$\rho_m$	=mean density, $=p_s m/RT_c$
$\mu$	=viscosity
$\mu_1$	=viscosity at maximum temperature
$\Phi$	=viscous dissipation function
$\Psi$	=stream function
$\psi$	=dimensionless stream function, $=\Psi/\rho_m V l$
$\omega$	=vorticity vector
$\Omega$	=dimensionless vorticity vector, $=\omega/(V/l)$
$\gamma$	=ratio of specific heats, $=c_p/c_v$
$\zeta$	=ratio of height to width, $=d/l$
$\eta$	=ratio of hot to cold temperature, $=T_h/T_c$

## Subscripts

c	=cold
d	=deviation from static pressure
e	=at the lower edge of the heater along the y axis
f	=at the upper edge of the heater along the y-axis
g	=at the very right of the heater along the x-axis
h	=hot
s	=static

## Superscript

'	=dimensionless
---	----------------

## References

- 1) Yatsuya, S., Kasukabe, S. and Uyeda. R.: Japanese J. Appl. Phys., 12, 1675 (1973).
- 2) Wilkes, J. O. and Churchill, S. W. : A.I.Ch.E. J., 12, 161 (1966).
- 3) Torrance, K. E. and Rockett, J. A. : J. Fluid Mech., 36, 33 (1969).
- 4) Davis, G. de V. : J. Heat Mass Transfer, 11, 1675 (1968).
- 5) Touloukian, Y. S., Saxena, S. C. and Hestermans, P. : "Thermophysical Properties of Matters, The TRPC Data Series", vol. II, (1970).
- 6) Touloukian, Y. S., P. E. Liley and S. C. Saxena. : "Thermophysical Properties of Matters, The TRPC Data Series", vol. III, (1970).
- 7) Richtmyer, R. D., : "Difference Methods for Initial Value Problems", Interscience Publishers Inc., New York (1957).